Comparison of Terrestrial Laser Scanning and X-ray Scanning in Measuring Scots Pine (Pinus sylvestris L.) Branch Structure

Pyörälä, Jiri

2018

Pyörälä , J , Kankare , V , Vastaranta , M , Rikala , J , Holopainen , M , Sipi , M , Hyyppä , J & Uusitalo , J 2018 , ' Comparison of Terrestrial Laser Scanning and X-ray Scanning in Measuring Scots Pine (Pinus sylvestris L.) Branch Structure ' , Scandinavian Journal of Forest Research , vol. 33 , no. 3 , pp. 291-298 . https://doi.org/10.1080/02827581.2017.1355409

http://hdl.handle.net/10138/233380
https://doi.org/10.1080/02827581.2017.1355409

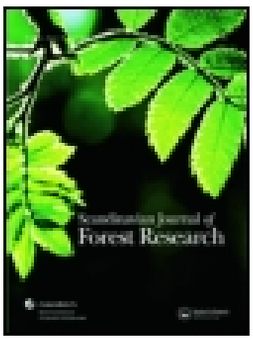

Scandinavian Journal of Forest Research

ISSN: 0282-7581 (Print) 1651-1891 (Online) Journal homepage: http://www.tandfonline.com/loi/sfor20

Comparison of terrestrial laser scanning and X-ray scanning in measuring Scots pine (Pinus sylvestris L.) branch structure

Jiri Pyörälä, Ville Kankare, Mikko Vastaranta, Juha Rikala, Markus Holopainen, Marketta Sipi, Juha Hyyppä & Jori Uusitalo

To cite this article: Jiri Pyörälä, Ville Kankare, Mikko Vastaranta, Juha Rikala, Markus Holopainen, Marketta Sipi, Juha Hyyppä & Jori Uusitalo (2017): Comparison of terrestrial laser scanning and X-ray scanning in measuring Scots pine (Pinus sylvestris L.) branch structure, Scandinavian Journal of Forest Research, DOI: 10.1080/02827581.2017.1355409

To link to this article: http://dx.doi.org/10.1080/02827581.2017.1355409

Accepted author version posted online: 14 Jul 2017.
Published online: 26 Jul 2017.

SCANDINAVIAN JOURNAL OF FOREST RESEARCH, 2017
https://doi.org/10.1080/02827581.2017.1355409

Taylor & Francis
Taylor & Francis Group

Comparison of terrestrial laser scanning and X-ray scanning in measuring Scots pine (*Pinus sylvestris* L.) branch structure

Jiri Pyörälä[a,b,c], Ville Kankare[a,b], Mikko Vastaranta[a,b], Juha Rikala[a], Markus Holopainen[a,b], Marketta Sipi[a], Juha Hyyppä[b,c] and Jori Uusitalo[d]

[a]Department of Forest Sciences, University of Helsinki, Helsinki, Finland; [b]Centre of Excellence in Laser Scanning Research, Finnish Geospatial Research Institute, Masala, Finland; [c]Department of Remote Sensing and Photogrammetry, Finnish Geospatial Research Institute, Masala, Finland; [d]Natural Resources Institute Finland (Luke), Parkano, Finland

ABSTRACT

While X-ray scanning is increasingly used to measure the interior quality of logs, terrestrial laser scanning (TLS) could be used to collect information on external tree characteristics. As branches are one key indicator of wood quality, we compared TLS and X-ray scanning data in deriving whorl locations and each whorl's maximum branch and knot diameters for 162 Scots pine (*Pinus sylvestris* L.) log sections. The mean number of identified whorls per tree was 37.25 and 22.93 using X-ray and TLS data, respectively. The lowest TLS-derived whorl in each sample tree was an average 5.56 m higher than that of the X-ray data. Whorl-to-whorl mean distances and the means of the maximum branch and knot diameters in a whorl measured for each sample tree using TLS and X-ray data had mean differences of −0.12 m and −6.5 mm, respectively. One of the most utilized wood quality indicators, tree-specific maximum knot diameter measured by X-ray, had no statistically significant difference to the tree-specific maximum branch diameter measured from the TLS point cloud. It appears challenging to directly derive comparative branch structure information using TLS and X-ray. However, some features that are extractable from TLS point clouds are potential wood quality indicators.

ARTICLE HISTORY
Received 4 November 2016
Accepted 2 July 2017

KEYWORDS
Ground-based LiDAR; wood quality; knots; wood procurement

Introduction

Highly detailed information on wood quality is considered essential for the optimization of wood procurement processes (Holopainen et al. 2014; Moore and Cown 2015). Sawmills plan their production before the trees are harvested, thus wood quality information on standing trees would allow harvesting wood of desired quantity and quality at the desired time instead of storing large amounts of wood onsite. The opportunity of determining the price of round wood according to its actual quality could also encourage private forest owners to grow high-quality wood if they were paid a premium based on wood quality (Malinen et al. 2010).

Wood quality refers to the performance and usability of wood as the end product (Moore and Cown 2015). Branches have a direct adverse effect on wood quality due to their high compression wood content and the distorted grain orientation around them (Mitsuhashi et al. 2008; Donaldson and Singh 2013). In addition, variation in branch characteristics is shown to correlate with variation in wood properties such as cell dimensions, cellular structure and wood density (Auty 2011; Cortini et al. 2013; Kuprevicius et al. 2013). Earlier research therefore aimed at developing methods for predicting wood quality using indicators of branchiness, most commonly the height of the lowest dead branch (H_{db}) (Kärkkäinen 1980; Uusitalo 1997; Lyhykäinen et al. 2009).

Single- or multidirectional industrial X-ray scanning (or X-ray tomography or X-ray digital radiography) is a method used at sawmills for assessing the wood quality of logs prior to their sawing (Oja et al. 2003). This method uses X-ray beams transmitted through an object, and the attenuation of the beams that penetrate the material are used to reconstruct a digital image of the measured object (Lechner et al. 2013). Whorl locations and dimensions are examples of parameters that can be measured using X-ray data and used to estimate the interior wood quality of a log (Grundberg and Grönlund 1997; Oja et al. 2004; Fredriksson 2012).

Terrestrial laser scanning (TLS) point clouds could potentially be used for measuring the wood quality factors of standing trees (Van Leeuwen et al. 2011). Kankare, Joensuu, et al. (2014) used TLS-derived diameter at breast height (DBH) and H_{db} for tree-specific wood quality estimations similarly to previous research (Kärkkäinen 1980; Uusitalo 1997; Lyhykäinen et al. 2009). Furthermore, several studies have presented automated modelling algorithms that enable the automatic measurements of tree stems (Thies et al. 2004; Henning and

CONTACT Jiri Pyörälä jiri.pyorala@helsinki.fi Departmentof Forest Sciences, University of Helsinki, Helsinki FI-00014, Finland; Centre of Excellence in Laser Scanning Research, Finnish Geospatial Research Institute, Masala FI-02431, Finland; Department of Remote Sensing and Photogrammetry, Finnish Geospatial Research Institute, Masala FI-02431, Finland

Radtke 2006; Liang et al. 2014; Olofsson et al. 2014), branches (Raumonen et al. 2013; Hackenberg et al. 2014) and bark properties or branch bumps (Kretschmer et al. 2013; Stängle et al. 2014) using TLS point cloud data. However, the downside of TLS is its limited spatial data coverage. Detailed wood quality information gathered by TLS could therefore be only applied to wood quality predictions of a particular stand at the time of its final felling or used to collect data for remote sensing-based estimations of wood quality in large areas (Maltamo et al. 2009; Hilker et al. 2013; Luther et al. 2013; Kankare, Vauhkonen, et al. 2014; Vastaranta et al. 2014).

To improve understanding of the potential of TLS in capturing external tree characteristics that are related to internal wood quality factors currently measurable by X-ray scanning, the aim of our study was to compare tree-specific wood quality measures (whorl number, whorl height, whorl-to-whorl distance and largest branch diameter of each whorl) derived from TLS data with respective measures derived from X-ray data. Branch diameter measured using TLS refers to the size of an external branch and knot diameter measured by X-ray scanning refers to the size of an internal branch: it is considered worthwhile to compare these slightly different diameters for revealing the possible dependencies. Additionally, TLS-derived DBH and H_{db} measurements were compared to those measured in the field.

Materials and methods

Study area and field measurements

The study material consisted of 180 Scots pine trees on four sample plots in Evo (61.19° N, 25.11° E) and two sample plots in Orimattila (60.80° N, 25.73° E), southern Finland, that is, 30 trees on each sample plot. Site fertility and growing stock information (m^3/ha) of the sample plots were based on existing stand-wise forest inventories from year 2013. DBH for the sample trees was measured using callipers in two perpendicular planes. Tree height (H) and H_{db} of the sample trees were measured using Vertex III (Haglöf, Sweden). The field measurements were carried out in August 2014.

The optical profile scanner device at the sawmill was used to measure the length of the saw log section (L_{log}), log top diameters (D_{top}) and log volumes (V_{log}) for each sample tree in September 2014. Sample plot and sample tree information is presented in Table 1 and Figure 1.

TLS data collection

TLS data were collected in August and September 2014 using a Faro Focus^{3D} X 330 (Faro Technologies Inc., USA) scanner that utilizes phase-shift technology. Trees were located in groups of six. Each group was scanned from 5 to 10 positions to obtain data coverage on all sides of every tree. Scan size was 10,310 rows and 4268 columns (44.0 M points). The point-to-point sampling distance was 6.3 mm at a 10 m distance. The point-to-point sampling distance variations from H_{db} to L_{log} height for each sample tree in each plot are presented in Table 2. The heights refer to the H_{db} measured in the field and the L_{log} measured at the sawmill (Table 1). The 3D distance from each scanning location to each tree at the mentioned heights was calculated using scanner location and tree location at breast height level.

Six spherical reference targets were used to register separate scans into a multi-scan point cloud. Spheres were 198.8 mm in diameter and they were set up on tripods at an approximate height of 1 m above ground. The spheres were distributed so that all spheres were visible during the first scan and a minimum of three spheres was visible during every other scan.

Preprocessing and registration of the scans was carried out using Faro Scene 5.2.1 software with inbuilt preprocessing and registration procedures. Preprocessing included filtering stray points using the 2D projection intensity map of the point cloud: the procedure inspects a point within a 3×3-pixel grid, and deletes the point if more than 50% of the other points within the grid are further than 2 cm from it. Points with a reflectance value less than 300 (on a scale of 0–2047) were filtered out. Examples of sample tree TLS point clouds are presented in Figure 2. The automatic registration procedure was carried out using the spheres as targets. The software evaluates the registration accuracy in terms of standard deviation of the target coordinates between the scans. The registration accuracy averaged 1.27 mm. Plot-specific variation in registration accuracy is presented in Table 2.

X-ray scanning data collection

The trees were harvested in September 2014 using the log-length logging method, that is, they were delimbed and topped at the saw log limit (D_{top} minimum 15 cm) in the forest and then hauled to the sawmill (Koskitukki, Kärkölä,

Table 1. Sample plot characteristics (VT = *Vaccinium* type, MT = *Myrtillus* type, OMT = *Oxalis-Myrtillys* type), mean stem volume of pine and other species per hectare (V_{Pine}/V_{other}) and sample tree statistics, mean values of diameter at breast height (DBH), height (H), height of the lowest dead branch (H_{db}), height of the live crown base (H_{lc}), length of the saw log section (L_{log}), log top diameter (D_{top}) and log volume (V_{log}).

	Sample plot characteristics		Sample tree statistics						
Plot	Site type	V_{Pine}/V_{other} (m^3/ha)	DBH (cm)	H (m)	H_{db} (m)	H_{lc} (m)	L_{log} (m)	D_{top} (cm)	V_{log} (m^3)
1	VT	220/10	28.9	22.6	4.8	14.4	15.5	15.6	0.6
2	VT	250/20	31.5	27.1	9.4	17.8	18.9	17.2	0.9
3	OMT	200/20	28.6	22.9	4.4	13.9	15.2	15.5	0.6
4	MT	140/260	35.5	28.9	8.2	20.9	18.6	18.5	1.0
5	MT	80/170	34.4	27.6	10.3	18.8	17.4	19.4	1.0
6	VT	170/80	31.4	25.8	7.4	15.5	15.3	18.5	0.7
Total		176.7/93.3	31.7	25.8	7.4	16.9	16.8	17.4	0.8

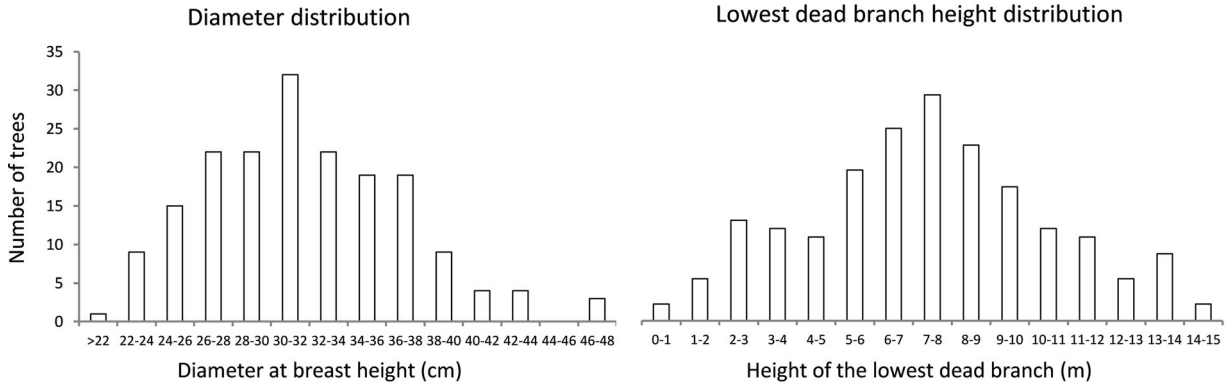

Figure 1. (Left) Diameter at breast height distribution (cm). (Right) Height distribution of the lowest dead branch (m) of the sample trees.

Finland). Before hauling, an ID number was marked on both ends of the stem to enable linking tree-specific field, TLS and X-ray measurements to each other.

The stems were scanned by a single-direction X-ray digital radiograph scanner Opmes AX1 (Inray, Finland). The scanning resolution was 2.5 mm/pixel in the longitudinal direction and 0.85 mm/pixel in the transversal direction. X-ray scanning was performed successfully for 162 of the 180 trees. The method was sensitive to any disturbances in the flow. No X-ray data were available for 14 trees due to halts and delays in the measurement process. In addition, four trees had data gaps and were thus excluded from further analyses.

TLS point cloud measurements of branches, branch bumps and DBH

Point cloud measurements were carried out using TerraScan software (TerraSolid, Finland) on the MicroStation V8i platform (Bentley Systems, USA). Stump height was visually estimated from the point cloud as the upper limit of the root collar. Whorls were identified visually. A slice of the branch base points perpendicular to the branch's longitudinal axis was extracted from the largest branch in each whorl. In order to exclude points belonging to the stem and to include a sufficient amount of points belonging to the branch, the extracted slice included points within a 2-to 12-cm distance from the stem (Figure 3, right).

The extracted branch base points were projected onto a plane perpendicular to the branch's longitudinal axis and the branch diameter was modelled by fitting a circle to the points using the random sample consensus (RANSAC) algorithm (Fischler and Bolles 1981). A random sample of three points was selected, to which a circle was initially fitted using ordinary least squares (OLS) approximation. Then, the ratio of points that lie within a certain threshold distance ($d = 1$ mm) from the circle arc (inliers) was calculated. The iteration was repeated N times to find a model that fits all the inliers with a certain probability P, as calculated using Equation (1) (Fischler and Bolles 1981):

$$N = \frac{\log(1-P)}{\log(1-p^n)}, \quad (1)$$

where p is the estimated ratio of inliers and n is the size of the random sample. Based on visual inspections the ratio of inliers among the extracted branch points could be as low as 0.2. Therefore, the following parameters were used in our study: $P = 0.99$, $p = 0.2$ and $n = 3$. The diameter of the circle fitted to the inliers from the best iteration round using OLS was considered as the branch diameter estimate. Whorl height was defined as the height difference between the stump and the centre of the fitted circle.

Self-pruned branches can appear on the stem surface as branch bumps before they are fully enclosed by stem wood. Visible branch bumps along the branchless part of the stem were visually identified and the height from the stump to the centre of the branch bump was measured using the MicroStation "Measure distance" tool (Figure 3, right).

Breast height level in the point cloud was defined at a 1.3-m height from the stump. DBH was measured by fitting a circle on a 2-cm thick horizontal slice of points at breast height level (1.29–1.31 m) using the same method as for the branch measurements.

Table 2. Point-to-point sampling distance and registration statistics for each sample plot.

	Point-to-point distance at the lowest dead branch height (mm)				Point-to-point distance at the log top height (mm)				Registration accuracy (mm)			
Plot	Min	Mean	Max	Std.	Min	Mean	Max	Std.	Min	Mean	Max	Std.
1	1.7	6.6	12.3	2.2	8.1	11.5	16.2	1.7	0.4	1.2	3.5	0.9
2	3.7	9.4	14.9	2.3	7.7	14.0	18.5	3.7	0.2	1.0	2.2	0.5
3	2.2	6.8	12.2	2.4	1.9	10.5	16.7	2.2	0.3	0.7	1.7	0.3
4	3.1	8.5	15.4	2.3	1.4	12.7	19.6	3.1	0.6	1.5	5.6	1.0
5	3.3	8.9	15.8	1.8	1.6	11.8	19.7	3.3	0.4	1.4	2.4	0.6
6	3.0	8.3	17.2	2.5	1.1	11.6	18.8	3.0	0.4	1.7	3.3	0.8
All	1.7	8.1	17.2	2.3	1.1	12.0	19.7	1.7	0.2	1.3	5.6	0.8

Figure 2. Examples of TLS point clouds of sample trees in this data set. The diameter at breast height (DBH) is indicated horizontally at breast height level (1.3 m from the ground). Height of the lowest dead branch (H_{db}) is indicated vertically with the inner right-hand-side number. Length of the saw log section (L_{log}) is indicated vertically with the outer right-hand-side number. (Left) A sample tree on plot 3, DBH 0.29 m, H_{db} 7.0 m, L_{log} 15.6 m. (Middle) A sample tree on plot 2, DBH 0.35 m, H_{db} 11.5 m, L_{log} 19.9 m. (Right) A sample tree on plot 4, DBH 0.25 m, H_{db} 18.7 m, L_{log} 12.1 m.

X-ray image measurements of knots

The X-ray images are constructed by converting the attenuation value of each beam into a grey-level (GL) value that is given to a respective pixel; the higher the attenuation, the higher the GL value. Whorls in the images are detected from the surrounding heartwood as they are denser and cause greater attenuation to the X-rays. Whorls cannot be detected in sapwood due to its high moisture content that

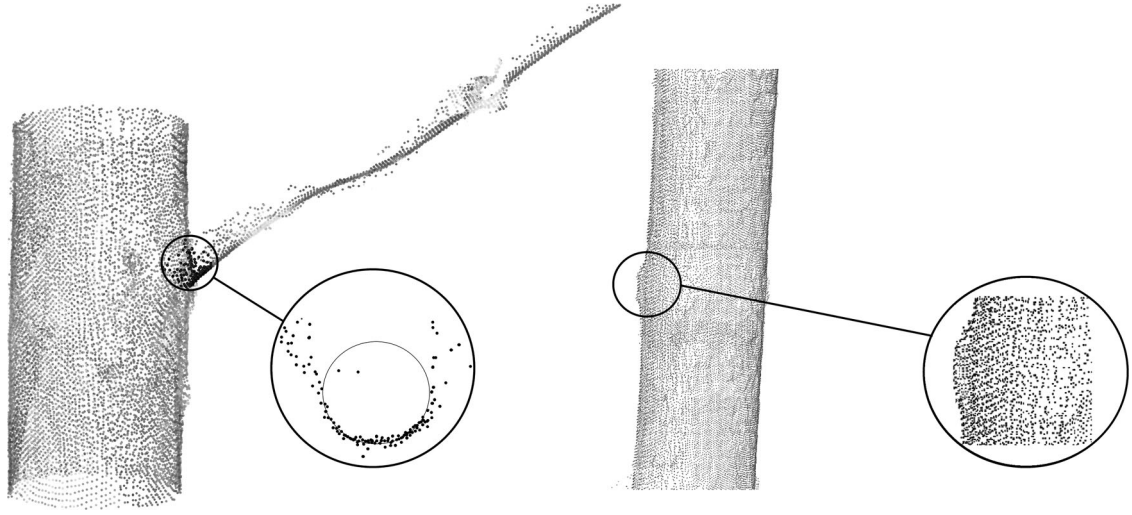

Figure 3. (Left) Example of branch detection and diameter measurements using TLS point clouds. Black points represent the branch base points that are extracted and projected onto a plane perpendicular to the branch's longitudinal axis (zoom). A circle is fitted around the points to estimate branch diameter. (Right) Example of branch bump detection, note the swelling around a self-pruned branch that is not yet fully enclosed (zoom).

causes greater scattering and attenuation of X-rays than in the heartwood.

In this study, Inray Co Ltd. analysed the X-ray images with their in-house software using a method that is used at sawmills. In this method, whorls in the 2D images were identified as pixels belonging to a group of local GL maxima. The maximum knot diameter of each whorl was estimated based on the maximum length of the group on a tree's longitudinal axis.

Whorls with a maximum knot diameter below 10 mm were excluded from the X-ray data. These whorls were found to be associated with small branches that had been self-pruned or to have such small branches that they could not be observed with the TLS when using the implemented settings.

Comparison of TLS-derived branch measurements to X-ray and field measurements

The comparison of TLS and X-ray data considered log sections only. Differences between the number of identified whorls, whorl heights, whorl-to-whorl distances and the diameters of the largest knot and branch per whorl measured with X-ray and TLS were compared using descriptive statistics including minimum, mean, maximum and standard deviation values for each tree.

A paired *t*-test was used to test whether the differences in the descriptive statistics between the TLS and X-ray data were statistically significant. The significance threshold was fixed to 0.05 for all statistics. The 95% confidence interval was also calculated for the difference in the given statistic between the data sets.

In a similar manner, DBH and the H_{db} measured in the TLS point cloud were compared to those measured in the field with callipers and a Vertex for each of the 180 trees.

Table 3. Descriptive statistics of whorl number, whorl heights, whorl-to-whorl distances and largest knot and branch diameters in a whorl for each sample tree using X-ray and TLS data.

X-ray: Whorl detection	$N = 162$ (the number of trees)			
	Min	Mean	Max	Standard deviation
Whorls detected	9	37.25	71	10.85
X-ray: Whorl heights (m)				
Min	0.15	1.68	6.72	1.20
Mean	2.95	8.80	13.69	2.11
Max	5.39	15.91	19.62	2.88
Standard deviation	1.63	4.19	5.77	0.79
X-ray: Whorl-to-whorl distance (m)				
Min	0.06	0.09	0.22	0.03
Mean	0.20	0.32	0.52	0.06
Max	0.31	0.77	3.12	0.36
Standard deviation	0.07	0.14	0.54	0.06
X-ray: Max knot diameter in a whorl (mm)				
Min	10.00	10.23	13.30	0.66
Mean	12.82	23.15	39.53	5.29
Max	18.30	48.64	93.30	15.96
Standard deviation	2.12	9.04	17.87	3.44
TLS: Whorl detection				
Whorls detected	6.00	22.93	51.00	7.99
TLS: Whorl heights (m)				
Min	0.83	7.24	17.51	2.78
Mean	6.97	12.26	19.48	2.27
Max	10.84	16.30	21.47	2.26
Standard deviation	0.90	2.64	4.57	0.72
TLS: Whorl-to-whorl distance (m)				
Min	0.04	0.19	0.60	0.09
Mean	0.23	0.44	1.01	0.12
Max	0.38	1.09	3.74	0.64
Standard deviation	0.03	0.21	0.73	0.14
TLS: Max branch diameter in a whorl (mm)				
Min	7.21	17.19	25.35	3.76
Mean	20.91	29.65	45.29	4.50
Max	26.32	49.06	115.37	16.30
Standard deviation	2.05	7.98	26.89	3.42

Results

An average of 37.25 whorls with the diameter of the largest knot exceeding 10 mm were identified in each sample tree log section using the X-ray data and 22.93 whorls per sample tree using the TLS data (Table 3). The mean difference between the methods was 14.9 whorls per tree, which was statistically significant according to the paired *t*-test ($p < .05$) (Table 4). Thus, 55% of the whorls within log sections with the largest knot diameter exceeding 10 mm identified with X-ray could also be detected using TLS point clouds (Tables 3 and 4).

Minimum whorl height averaged 1.67 m in the X-ray data and 7.24 m in the TLS data (Table 3), and the mean difference between minimum whorl heights was −5.56 m for each of the sample trees (Table 4). The difference between the data sets was statistically significant according to the paired *t*-test ($p < .05$) (Table 4).

Mean whorl-to-whorl distance of the sample trees was 0.32 and 0.44 m according to the X-ray and TLS methods, respectively (Table 3). The mean difference between the TLS- and X-ray-derived mean whorl-to-whorl distances for each sample tree was −0.11 m (Table 4). The difference between the data sets was statistically significant according to the paired *t*-test ($p < .05$) (Table 4).

The tree-specific mean of the maximum knot diameter for each whorl was 23.2 mm according to the X-ray method and the tree-specific mean of the maximum branch diameter for each whorl was 29.7 mm according to the TLS method (Table 3). The mean difference between the X-ray-derived mean of the maximum knot diameter in each whorl and TLS-derived mean of the maximum branch diameter in each whorl for each sample tree averaged −6.49 mm (Table 4). The difference between the data sets was statistically significant according to the paired *t*-test ($p < .05$) (Table 4).

The mean of the maximum knot size for each sample tree was 48.7 mm according to the X-ray method and the mean of the maximum branch size was 49.1 mm according to the TLS method (Table 4). The difference between the maximum knot size in the X-ray data and the maximum branch size in the TLS data was −0.42 mm and it was not statistically significant ($p = .79$) (Table 4).

Mean H_{db} was 7.27 m according to the TLS method and 7.40 m according to the field measurements. Mean DBH

Table 4. Descriptive and paired *t*-test statistics of the differences for each sample tree in terms of the number of whorls, whorl heights, whorl-to-whorl distance and knot and branch diameter measurements between X-ray and TLS data, respectively: minimum, mean, maximum and standard deviation (Std.) values and the *t*-statistic, degrees of freedom (df), *p*-value and 95% confidence intervals.

$N = 162$ (the number of trees) Whorl detection	Min	Mean	Max	Std.	*t*-statistic	df	*p*-value	95% conf. int.	
Whorls	−22.00	14.07	51.00	12.38	14.46	161	<.05	12.15	15.99
Whorl height (m)									
Min	−17.17	−5.56	0.62	2.90	−24.40	161	<.05	−6.01	−5.11
Mean	−8.17	1.56	8.99	2.78	−21.09	161	<.05	−3.78	−3.14
Max	−3.61	8.67	17.47	3.32	−1.88	161	<.05	−0.78	0.02
Std.	−12.25	−3.05	3.53	2.70	20.08	161	<.05	1.40	1.70
Whorl-to-whorl distance (m)									
Min	−0.49	−0.10	0.07	0.09	−14.84	161	<.05	−0.12	−0.09
Mean	−0.64	−0.11	0.10	0.11	−13.46	161	<.05	−0.13	−0.10
Max	−2.94	−0.32	2.20	0.74	−5.53	161	<.05	−0.44	−0.21
Std.	−0.61	−0.07	0.39	0.16	−5.39	161	<.05	−0.09	−0.04
Diameter (mm)									
Min	−15.35	−6.96	4.49	3.86	−22.97	161	<.05	−7.56	−6.37
Mean	−23.10	−6.49	6.68	5.30	−15.59	161	<.05	−7.32	−5.67
Max	−74.02	−0.42	43.50	19.95	−0.27	161	.79	−3.51	2.68
Std.	−18.92	1.06	10.11	4.30	3.14	161	<.05	0.39	1.73

was 31.70 cm according to the TLS method and 31.45 cm according to the field measurements. Mean differences between H_{db} and DBH measured in the field and using TLS for each sample tree were 1.05 m with a standard deviation of 1.60 m and 0.69 cm with a standard deviation of 0.67 cm, respectively.

Discussion

In our study, we compared the TLS and X-ray scanning measurements of Scots pine branch and knot structure. The results might have been affected by the following factors: The X-ray data was obtained from single-directional X-ray scanning, which can account for the occlusion of certain whorls due to noise in the reconstruction images caused by wood density variations among the growth rings and possible cracks or decay (Oja et al. 2004). In addition, the largest knot diameter in a whorl was estimated as the length of the whorl along the stems longitudinal axis in the X-ray images, which is sensitive to noise and overlapping knots. In TLS, visual whorl identification may be prone to subjective errors depending on the carefulness and experience of the measurer, especially in cases of diminishing point cloud quality towards the tree tops. The point divergence varied, on average, from 8.1 mm (height of the lowest dead branch) to 12.0 mm (height of the log top) for each sample tree (Table 2), which may have affected the identification of small-branched whorls, in particular. In addition, occlusion caused by the crown is likely to have affected whorl identification. Registration error (mean of 1.27 mm) between the scans might have caused small errors in the branch diameter measurements (Table 2). Moreover, distortions in some TLS point clouds due to wind might have affected the accuracy of the branch diameter measurements to a much greater extent, especially towards the tree tops where the effect of wind was at its greatest (Vaaja et al. 2016).

Based on the whorl height statistics (Table 3), most of the difference in the number of identified whorls between the methods was caused by the knots in the lower parts of the tree that are detected using X-ray data, but that have no external branches identifiable using the TLS data (Tables 3 and 4).

Measurements of tree's radial growth are found to improve wood quality estimation, as reported in previous studies by Björklund and Petersson (1999) and Uusitalo and Isotalo (2005). However, growth ring measurements are not possible without drilling or tree felling, and thus an alternative way for measuring the tree growth in standing trees is needed. As the radial growth of one year and the height growth of the following year have been found to correlate by for example, Mäkinen (1998) and Salminen et al. (2009), the possibility of using height growth instead of radial growth in wood quality estimations should be subjected to further studies. Mean tree-specific whorl-to-whorl distances should be a close proxy for the mean annual height growth and were therefore compared between the data sets. The results showed that the whorl-to-whorl distances in TLS tend to be overestimations compared to the whorl-to-whorl distances detected by the X-ray (Table 4).

The mean of the maximum branch diameters in a whorl for each sample tree in the TLS data was higher than the respective mean in the X-ray data (Table 3). The difference is probably explained by the measurement inaccuracies prevalent in either data set, but also by the higher mean whorl height in the TLS data: the share of living branches increases towards the tree tops and increases the discrepancy between internal knot and external branch diameters.

Björklund and Petersson (1999) have concluded that the maximum knot size within a Scots pine log is a robust indicator of the overall knottiness of the log. In our study, the mean difference between the tree-specific maximum knot diameter measured using X-ray scanning and the tree-specific maximum branch diameter measured using TLS was not statistically significant (Table 4).

When we compared TLS-derived and field-measured DBH and H_{db}, the obtained mean differences and standard deviations of the differences were in line with previous studies

such as Kankare, Joensuu, et al. (2014) and Olofsson et al. (2014). These variables have previously been used for wood quality estimations in for example, Uusitalo (1997).

In conclusion, the branch structures derived using TLS and X-ray scanning data are not directly comparable with each other, due to the differences between external and internal tree characteristics and between the measurement techniques themselves. However, some branch structure features that are extractable from TLS point clouds, for example, the maximum branch size and height of the lowest dead branch, are potential indicators of wood quality as previously suggested (Kärkkäinen 1980; Uusitalo 1997; Björklund and Petersson 1999). TLS is among the novel, emerging techniques for measuring trees' external structures in increasing detail. Moreover, automated stem and branch recognition and modelling algorithms have been developed to further enhance the tree attribute analysis process on point clouds (Raumonen et al. 2013; Hackenberg et al. 2014; Liang et al. 2014). This development can result in new assessment methods for the wood quality of standing trees.

Acknowledgements

Evo forest school is acknowledged for providing their facilities and the forest plots to our use. The reference data from optical and X-ray sources were provided by the courtesy of Koskitukki co ltd., Janne Kovanen from Inray co ltd. and from the VARMA-project carried out by the Technical Research Centre of Finland (special thanks to Hannu Rummukainen and Marika Makkonen). The authors also acknowledge Olli Ylhäisi and Pekka Helminen for their cooperation and for coordinating the collection of reference and field measurement data. The language was edited by Stella Thompson.

Disclosure statement

No potential conflict of interest was reported by the authors.

Funding

This work was supported by the Academy of Finland project "Centre of Excellence in Laser Scanning Research" (CoE-LaSR) [272195], the Ministry of Agriculture and Forestry of Finland project "Puuston laatutunnukset" [OH300-S42100-03], the Foundation for Research of Natural Resources in Finland [1780/15, 1790/16 and 1798/17] and the Finnish Forest Foundation [2014092904]. This work was also supported by Jenny ja Antti Wihurin Rahasto.

References

Auty D. 2011. Modelling the effects of forest management on the wood properties and branch characteristics of UK-grown Scots pine [dissertation]. Aberdeen: University of Aberdeen.

Björklund L, Petersson H. 1999. Predicting knot diameter of *Pinus Sylvestris* in Sweden. Scand J Forest Res. 14:376–384.

Cortini F, Groot A, Filipescu CN. 2013. Models of the longitudinal distribution of ring area as a function of tree and stand attributes for four major Canadian conifers. Ann Forest Sci. 70:637–648.

Donaldson LA, Singh AP. 2013. Formation and structure of compression wood. Plant Cell Monogr. 20:225–256.

Fischler MA, Bolles RC. 1981. Random sample consensus: a paradigm for model fitting with applications to image analysis and automated cartography. Commun ACM. 24:381–395.

Fredriksson M. 2012. Reconstruction of *Pinus Sylvestris* knots using measurable log features in the Swedish pine stem bank. Scand J Forest Res. 27:481–491.

Grundberg S, Grönlund A. 1997. Simulated grading of logs with an X-Ray log scanner – grading accuracy compared with manual grading. Scand J Forest Res. 12:70–76.

Hackenberg J, Morhart C, Sheppard J, Spiecker H, Disney M. 2014. Highly accurate tree models derived from terrestrial laser scan data: a method description. Forests. 5:1069–1105.

Henning JG, Radtke PJ. 2006. Detailed stem measurements of standing trees from ground-based scanning LiDAR. Forest Sci. 52:67–80.

Hilker T, Frazer GW, Coops NC, Wulder MA, Newnham GJ, Stewart JD, van Leeuwen M, Culvenor DS. 2013. Prediction of wood fiber attributes from LiDAR-derived forest canopy indicators. Forest Sci. 59:231–242.

Holopainen M, Vastaranta M, Hyyppä J. 2014. Outlook for the next generation's precision forestry in Finland. Forests. 5:1682–1694.

Kankare V, Joensuu M, Vauhkonen J, Holopainen M, Tanhuanpaa T, Vastaranta M, Hyyppa J, Hyyppa H, Alho P, Rikala J, et al. 2014. Estimation of the timber quality of Scots pine with terrestrial laser scanning. Forests. 5:1879–1895.

Kankare V, Vauhkonen J, Tanhuanpaa T, Holopainen M, Vastaranta M, Joensuu M, Krooks A, Hyyppa J, Hyyppa H, Alho P, et al. 2014. Accuracy in estimation of timber assortments and stem distribution - a comparison of airborne and terrestrial laser scanning techniques. ISPRS J Photogramm. 97:89–97.

Kärkkäinen M. 1980. Mäntytukkirunkojen Laatuluokitus. Summary: grading of Pine Sawlog stems. Commun Inst For Fenn. 96:1–152.

Kretschmer U, Kirchner N, Morhart C, Spiecker H. 2013. A new approach to assessing tree stem quality characteristics using terrestrial laser scans. Silva Fenn. 47:1–14.

Kuprevicius A, Auty D, Achim A, Caspersen JP. 2013. Quantifying the influence of live crown ratio on the mechanical properties of clear wood. Forestry. 86:361–369.

Lechner T, Sandin Y, Kliger R. 2013. Assessment of density in timber using X-Ray equipment. Int J Archit Herit. 7:416–433.

Liang XL, Kankare V, Yu XW, Hyyppä J, Holopainen M. 2014. Automated stem curve measurement using terrestrial laser scanning. IEEE T Geosci Remote. 52:1739–1748.

Luther JE, Skinner R, Fournier RA, van Lier OR, Bowers WW, Coté J-F, Hopkinson C, Moulton T. 2013. Predicting wood quantity and quality attributes of balsam fir and black spruce using airborne laser scanner data. Forestry. 10.1093/forestry/cpt039.

Lyhykäinen HT, Mäkinen H, Mäkela A, Pastila S, Heikkila A, Usenius A. 2009. Predicting lumber grade and by-product yields for Scots pine trees. Forest Ecol Manag. 258:146–158.

Mäkinen H. 1998. The suitability of height and radial increment variation in *Pinus Sylvestris* (L.) for expressing environmental signals. Forest Ecol Manag. 112:191–197.

Malinen J, Berg V, Kilpeläinen H. 2010. Roundwood pricing mechanisms and their performance in Scots pine roundwood markets. Working papers of the Finnish Forest Research Institute. 147:35.

Maltamo M, Peuhkurinen J, Malinen J, Vauhkonen J, Packalén P, Tokola T. 2009. Predicting tree attributes and quality characteristics of Scots pine using airborne laser scanning data. Silva Fenn. 43:507–521.

Mitsuhashi K, Poussa M, Puttonen J. 2008. Method for predicting tension capacity of sawn timber considering slope of grain around knots. J Wood Sci. 54:189–195.

Moore J, Cown D. 2015. Wood quality variability – what is it, what are the consequences and what we can do about it? NZ J For. 59:1–3.

Oja J, Grundberg S, Fredriksson J, Berg P. 2004. Automatic grading of sawlogs: a comparison between X-Ray scanning, optical three-dimensional scanning and combinations of both methods. Scand J Forest Res. 19:89–95.

Oja J, Wallbäcks L, Grundberg S, Hägerdal E, Grönlund A. 2003. Automatic grading of Scots pine (*Pinus Sylvestris* L.) sawlogs using an industrial X-Ray log scanner. Comput Electron Agric. 41:63–75.

Olofsson K, Holmgren J, Olsson H. 2014. Tree stem and height measurements using terrestrial laser scanning and the Ransac algorithm. Remote Sens-Basel. 6:4323–4344.

Raumonen P, Kaasalainen M, Akerblom M, Kaasalainen S, Kaartinen H, Vastaranta M, Holopainen M, Disney M, Lewis P. 2013. Fast automatic precision tree models from terrestrial laser scanner data. Remote Sens-Basel. 5:491–520.

Salminen H, Jalkanen R, Lindholm M. 2009. Summer temperature affects the ratio of radial and height growth of Scots pine in northern Finland. Ann Forest Sci. 66:810–810.

Stängle SM, Bruchert F, Kretschmer U, Spiecker H, Sauter UH. 2014. Clear wood content in standing trees predicted from branch scar measurements with terrestrial LiDAR and verified with X-ray computed tomography. Can J Forest Res. 44:145–153.

Thies M, Pfeifer N, Winterhalder D, Gorte BG. 2004. Three-dimensional reconstruction of stems for assessment of taper, sweep and lean based on laser scanning of standing trees. Scand J Forest Res. 19:571–581.

Uusitalo J. 1997. Pre-harvest measurement of pine stands for sawing production planning. Acta Forestalia Fennica. 259:1–56.

Uusitalo J, Isotalo J. 2005. Predicting knottiness of pinus sylvestris for use in tree bucking procedures. Scand J Forest Res. 20:521–533.

Vaaja M, Virtanen J-P, Kurkela M, Lehtola V, Hyyppä J, Hyyppä H. 2016. The effect of wind on tree stem parameter estimation using terrestrial laser scanning. ISPRS Annals. III-8:117–122.

Van Leeuwen M, Hilker T, Coops NC, Frazer G, Wulder MA, Newnham GJ, Culvenor DS. 2011. Assessment of standing wood and fiber quality using ground and airborne laser scanning: a review. Forest Ecol Manag. 261:1467–1478.

Vastaranta M, Saarinen N, Kankare V, Holopainen M, Kaartinen H, Hyyppa J, Hyyppa H. 2014. Multisource single-tree inventory in the prediction of tree quality variables and logging recoveries. Remote Sens-Basel. 6:3475–3491.